Biol Blood Marrow Transplant 20 (2014) 760–769

Biology

# Collateral Damage of Nonhematopoietic Tissue by Hematopoiesis-Specific T Cells Results in Graft-versus-Host Disease During an Ongoing Profound Graft-versus-Leukemia Reaction

Boris van der Zouwen, Alwine B. Kruisselbrink, J.H. Frederik Falkenburg, Inge Jedema*

*Department of Hematology, Leiden University Medical Center, Leiden, The Netherlands*

*Article history:*
Received 27 December 2013
Accepted 1 March 2014

*Key Words:*
Allogeneic stem cell transplantation
Graft-versus-host disease
Collateral damage
T cell
Minor histocompatibility antigen

A B S T R A C T

After allogeneic stem cell transplantation (allo-SCT), donor T cells may recognize minor histocompatibility antigens (MiHA) specifically expressed on cells of the recipient. It has been hypothesized that T cells recognizing hematopoiesis-restricted MiHA mediate specific graft-versus-leukemia (GVL) activity without inducing graft-versus-host disease (GVHD), whereas T cells recognizing ubiquitously expressed MiHA induce both GVL and GVHD reactivity. It also has been hypothesized that alloreactive CD4 T cells are capable of mediating specific GVL reactivity due to the hematopoiesis-restricted expression of HLA class II. However, clinical observations suggest that an overt GVL response, associated with expansion of T cells specific for hematopoiesis-restricted antigens, is often associated with GVHD reactivity. Therefore, we developed in vitro models to investigate whether alloreactive T cells recognizing hematopoiesis-restricted antigens induce collateral damage to surrounding nonhematopoietic tissues. We found that collateral damage to MiHA-negative fibroblasts was induced by misdirection of cytotoxic granules released from MiHA-specific T cells activated by MiHA-positive hematopoietic cells, resulting in granzyme-B–mediated activation of apoptosis in the surrounding fibroblasts. We demonstrated that direct contact between the activated T cell and the fibroblast is a prerequisite for this collateral damage to occur. Our data suggest that hematopoiesis-restricted T cells actively participate in an overt GVL response and may contribute to GVHD via induction of collateral damage to nonhematopoietic targets.



## INTRODUCTION

The graft-versus-leukemia/lymphoma (GVL) effect after HLA-matched allogeneic stem cell transplantation (allo-SCT) [1,2] mediated by donor T cells recognizing minor histocompatibility antigens (MiHAs) [3-5] expressed on malignant cells of the recipient is the major beneficial therapeutic effect of allo-SCT [2-8]. It has been hypothesized that donor T cells recognizing MiHA expressed ubiquitously on both hematopoietic and nonhematopoietic tissues are involved in combined GVL and graft-versus-host disease (GVHD) responses, whereas immune responses directed against hematopoiesis-restricted MiHAs give rise to specific GVL reactivity without coinciding GVHD.

Because HLA-DP is often not taken into account in the donor search (10/10 HLA match), alloreactive donor T cells directed against the mismatched HLA-DP allele(s) may contribute to the GVL effect. Given that under normal conditions, the expression of HLA class II is restricted to hematopoietic cells, it has been hypothesized that CD4 T cells are capable of mediating a specific GVL effect without coinciding GVHD [9-11]; however, mismatching for hematopoiesis-restricted antigens, such as HA-1, in the allo-SCT setting has been associated with a higher incidence of GVHD [12,13]. In accordance with these clinical observations, in situ analysis of the GVHD reactivity of HA-1– and HA-2–specific T cells in skin explant models revealed modest (grade II) GVHD induction [14]. Moreover, we and others have observed that after donor lymphocyte infusion (DLI), induction of a profound GVL response accompanied by amplification of T cell responses against hematopoiesis-restricted antigens often coincides with limited, mainly skin, GVHD.

Alloimmune responses after transplantation are unlikely to be of single specificity, and thus the contribution of single T cell responses cannot be precisely determined; nonetheless, these observations may indicate a less stringent separation between the tissue-specific expression of targeted antigens and development of GVHD. We hypothesized that under specific conditions, T cells directed against hematopoiesis-restricted antigens may induce damage to nonhematopoietic targets, possibly via the induction of collateral damage or bystander lysis to nonhematopoietic cells, while targeting the malignant/hematopoietic cells.

In 1986, using an in vitro model, Lanzavecchia et al. [15] demonstrated that cytotoxic T lymphocytes (CTLs) triggered by recognition of their specific target can kill other cells that are not directly recognized by the T cells but are in close contact with the triggered T cells. Furthermore, the capacity of virus- and tumor-specific CD8/CD4 T cells to induce collateral damage to neighboring bystander cells has been demonstrated using in vitro models [16-18]. Conflicting reports on the cytotoxic effector mechanisms underlying this phenomenon have been published [15,16,19-25].

The aim of the present study was to investigate whether and under what conditions T cells recognizing hematopoiesis-restricted antigens (MiHAs or allo-HLA) may be able to induce

*Financial disclosure:* See Acknowledgments on page 769.

* Correspondence and reprint requests: Dr. Inge Jedema, Department of Hematology, Leiden University Medical Center, C2R-140, PO Box 9600, 2300 RC Leiden, The Netherlands.
*E-mail address:* i.jedema@lumc.nl (I. Jedema).

1083-8791/$ – see front matter © 2014 American Society for Blood and Marrow Transplantation.
http://dx.doi.org/10.1016/j.bbmt.2014.03.002

damage to nonhematopoietic targets and thereby contribute to the GVHD response seen in profound GVL responses after allo-SCT or DLI. To address this question, we developed in vitro models mimicking the complex immunologic conditions after allo-SCT. Our data suggest that under circumstances in which the magnitude of the immune response dictates the formation of a local proinflammatory environment leading to up-regulation of adhesion molecules on the surrounding tissue cells, hematopoiesis-restricted antigen-specific T cells can interact with and, when simultaneously antigen-specifically activated by hematopoietic (tumor) cells, damage the surrounding nonhematopoietic cells. This phenomenon may result in local development of GVHD or may amplify GVHD reactivity during a profound GVL response without direct antigen-specific recognition of the nonhematopoietic cells by the T cells.

## MATERIALS AND METHODS

### *Fibroblasts*

After informed consent was provided, primary human fibroblasts were generated from skin biopsy specimens obtained from patients or healthy donors. The skin biopsy specimens were washed with PBS, minced, and then transferred to 6-well culture plates containing low-glucose DMEM (Lonza, Verviers, Belgium) supplemented with 10% FBS (Life Technologies, Breda, The Netherlands). Fibroblasts were cultured to 90% confluency and then harvested using trypsin (Lonza) for 7 minutes at 37 °C, followed by 2 washes. Stock samples were cryopreserved in liquid nitrogen. After thawing, the samples were reseeded at a concentration of 5000 cells/cm$^2$ and recultured to 90% confluency, harvested, and reseeded. Experiments were performed using fibroblasts cultured for 5-20 passages. In specific experiments, fibroblasts were pretreated for 2 days with IFN-γ (200 IU/mL; Boehringer Ingelheim, Alkmaar, The Netherlands). For specific experiments, fibroblasts were retrovirally transduced with pLZRS constructs encoding CD54, BCL-2, PI9, c-FLIP, or empty vector (mock), linked to the truncated human nerve growth factor receptor (NGFR) or green fluorescent protein (GFP) selection marker gene via an internal ribosome entry site (IRES) sequence [26-28]. The identity of all constructs was verified by sequencing. Retroviral supernatants were generated with phoenix packaging (Φ-NX-A) cells, as described previously [29], and used for transduction of fibroblasts using recombinant human fibronectin fragments (CH-296; Lonza). Mock-, BCL-2–, and PI-9-GFP–transduced fibroblasts were purified by flow cytometry cell sorting, and mock-, CD54-, PI-9–, and c-FLIP-NGFR–transduced fibroblasts were stained with NGFR-PE and purified by magnetic-activated cell sorting (MACS) using anti-PE beads (Miltenyi Biotec, Bergisch Gladbach, Germany) and/or flow cytometry cell sorting.

### *Stimulator Cells*

After informed consent was provided, peripheral blood samples were obtained from healthy individuals, and peripheral blood mononuclear cells (PBMCs) were isolated by Ficoll-isopaque separation and cryopreserved. Stable Epstein-Barr virus (EBV)-transformed B cell lines (EBV-LCLs) were generated as described previously and cultured in Iscove's modified Dulbecco's medium (IMDM; Lonza) supplemented with 10% FBS. Monocytes were isolated from donor PBMCs by MACS isolation using magnetic CD14 CliniMACS beads (Miltenyi Biotec) and then transformed into immature dendritic cells (DCs) by culturing for 2 days at a concentration of $10^6$ cells/mL in IMDM containing 10% prescreened human serum supplemented with 100 ng/mL granulocyte-macrophage colony stimulating factor (GM-CSF; Novartis, Basel, Switzerland) and 500 IU/mL IL-4 (kindly provided by Schering-Plough, Innishammon, Ireland), followed by 2 days of maturation using a cytokine mixture containing 100 ng/mL GM-CSF, 10 ng/mL IL-1β (Cellgenix, Freiburg, Germany), 10 ng/mL IL-6 (Cellgenix), 10 ng/mL TNF-α (Boehringer Ingelheim), 500 IU/mL IFN-γ (Immukine; Boehringer Ingelheim), and 1 μg/mL prostaglandin E2 (Sigma-Aldrich, Zwijndrecht, The Netherlands) to obtain mature monocyte-derived DCs [30,31]. Acute lymphoblastic leukemia (ALL) cell lines previously established in our laboratory from primary leukemic cells were cultured in serum-free medium as described previously [32].

### *Generation and Culture of T Cell Clones and Primary T Cell Populations*

The cytotoxic CD8$^+$ T cell clone (CTL) RDR2, specific for the HLA-A*0201–restricted MiHA LB-ADIR-1F, was previously isolated from peripheral blood of a patient at the time of clinical response to DLI as treatment for relapsed multiple myeloma [33]. The HLA-A*0201–restricted SMCY$_{311-319}$-HY–specific CTL was isolated from a female patient after rejection of a male stem cell graft [34]. The allo-HLA-A*0201–specific CTL MBM13 was isolated in vitro from an HLA-A*0201–mismatched mixed lymphocyte reaction. The HLA-A*0201–restricted HA-1–specific CTL was isolated from a patient who mounted a GVL response after allo-SCT with an HA-1–negative donor [35]. The CD4$^+$ T cell clones specific for HLA-DP2 or HLA-DP3 were isolated from a patient who mounted a GVL response after allo-SCT with an HLA-DP–mismatched donor [36]. The T cell clones were expanded in expansion-medium consisting of IMDM supplemented with 5% FBS, 5% prescreened pooled human serum, and 100 IU/mL IL-2 (Chiron, Amsterdam, The Netherlands). CTLs were restimulated using a feeder mixture containing expansion medium supplemented with 5× irradiated (50 Gy) allogeneic PBMCs and 0.2× irradiated (50 Gy) allogeneic EBV-LCL, and 0.8 μg/mL phytohemagglutinin (PHA)-HA16 (Remel, Dartford, UK) every 3 weeks. T cells were used for functional tests at 2-3 weeks after restimulation. Primary T cells were obtained from donor PBMCs using the Pan T Cell Isolation Kit II (Miltenyi Biotec), followed by positive selection of CD4- or CD8-naïve (CD45RA$^+$, CD27$^+$) and memory (CD45RO$^+$) T cells by flow cytometry.

### *Antibodies, Tetramers, and Flow Cytometry Analysis*

The FITC-labeled mAbs against CD4, CD19, CD27, CD107a, and HLA-A*0201; the PE-labeled mAbs against CD19, CD90, HLA-A*02, annexin V, and NGFR; the cyanin dye 7–coupled R-PE (PE-Cy7)-labeled mAb against CD3; and the allophycocyanin-labeled mAbs against CD137 and CD8 were obtained from BD Bioscience (San Jose, CA). CD90-FITC was obtained from Beckman Coulter (Fullerton, CA). CD45RA-PE Texas red–labeled mAb was obtained from Life Technologies. CD45RO-Alexa Fluor 700–labeled mAb was obtained from ITK/Biolegend (Uithoorn, The Netherlands). Allophycocyanin- or PE-labeled HLA-A*0201 tetramers containing the miHAs LB-ADIR-1F, HA-1, and SMCY-HY were constructed as described previously [37].

For surface molecule staining, cells were labeled with mAbs for 30 minutes at 4°C in PBS supplemented with 2% pasteurized plasma protein solution (Sanquin, Amsterdam, The Netherlands). Identity of the CTL clones was checked using surface staining with fluorescent-labeled HLA-A*0201 tetramers containing the miHA peptide [37].

### *Analysis of T Cell Activation and Degranulation*

T cell stimulation was performed by exposing 10,000 CTLs to different T cell stimulators, including PHA 800 ng/mL, anti–CD3-CD28 beads (T cell/bead ratio 10/1; Dynabeads, Life Technologies), EBV-LCL, ALL, monocytes, and immature and mature DCs (T cell/stimulator ratio 1/3). Supernatants were harvested after 4 hours and 24 hours, and IFN-γ release was measured by standard ELISA (Sanquin). Granzyme-B release and perforin release were measured in the same supernatants using human granzyme-B and perforin ELISA kits (Abcam, Cambridge, MA). In specific experiments, target cells were exogenously loaded with different concentrations (ranging from 1 pM to 1 μM) of the relevant MiHA peptides (SVAPALALFPA;LB-ADIR-1F, VLHDDLLEA;HA-1, or FIDSYICQV;SMCY-HY) for 1 hour at 37 °C.

### *Analysis of T Cell–Mediated Cytotoxicity*

For quantitative fluorescence-activated cell sorting (FACS) analysis of cytotoxicity [26], cells were taken up in 75 μL of PBS/2% pasteurized plasma protein solution after surface Ab staining. Shortly before the FACS analysis, 10,000 Flow-Count beads (Beckman Coulter) and propidium iodide (PI) were added. For each sample, 2000 beads were acquired. The numbers of viable fibroblasts were calculated by correcting the analyzed numbers of CD90$^+$, PI$^-$ cells for the number of beads. In specific experiments, cytotoxicity was examined in the presence or absence of blocking anti-intercellular adhesion molecule 1 (ICAM-1) mAbs (CD54, 5 ng/mL; ITK/Biolegend).

An annexin V apoptosis detection kit (BD Bioscience) was used for apoptosis analysis. In brief, cells were resuspended in 50 μL of binding buffer after surface Ab staining, after which annexin V-PE (1:50 dilution) and 2.5 μL of 7AAD were added, followed by a 15-minute incubation at 4 °C.

### *Confocal Microscopy*

Primary human fibroblasts (except for GFP-transduced fibroblasts) were labeled with 5 μM PKH67 according to manufacturer's instructions (Sigma-Aldrich) and seeded at 50,000 cells per glass bottom dish (P35G-1.5-14-C; MatTek, Ashland, MA) and cultured in DMEM without phenol red (Lonza; Life Technologies) supplemented with 10% FCS. After 3 days, medium was removed, and the adherent cells were washed 3 times with IMDM without phenol red (Lonza; Life Technologies) supplemented with 10% FCS. CTLs were labeled with 5 μM PKH26 according to the manufacturer's instructions (Sigma-Aldrich), and added to the fibroblasts at a 3/1 CTL/fibroblast ratio in IMDM without phenol red supplemented with 10% FCS and IL-2 (30 IU/mL). Hematopoietic stimulator cells were labeled with 5 μM Claret Far Red Fluorescent Cell Linker Kit (CellVue) according to the manufacturer's instructions (Sigma-Aldrich). PHA (800 ng/mL) or hematopoietic stimulator cells were added to the cultures (CTL/stimulator ratio 1/3). The dishes were incubated for different time intervals at 37°C, followed by confocal microscopy analysis

using a 488-nm laser (TCS SP5 confocal microscope; Leica Microsystems, Heidelberg, Germany). Fibroblast viability was analyzed using red dead cell staining (SYTOX; Life Technologies) according to the manufacturer's instructions. SYTOX (1/100 dilution) was added 15 minutes before visualization. Images were analyzed using Leica confocal software and ImageJ.

***Western Blot Analysis***

For each sample, $10^7$ cells were lysed in Triton lysis buffer as described previously [27,28,38]. Equal amounts of cell lysates were separated on SDS-PAGE gels, blotted onto PVDF membranes (Millipore, Bedford, MA), and blocked with 5% BSA in PBS/Tween 0.05% (Sigma-Aldrich). Monoclonal mouse anti-human Bcl-2 was purchased from Dako (Heverlee, Belgium; clone 124), mouse anti-human PI-9 was purchased from Serotec (Duesseldorf, Germany; clone 7D8), and mouse anti-human β-actin (AC-15) was purchased from Sigma-Aldrich. The mouse anti-human c-FLIP mAb NF6 was a kind gift from P. H. Krammer (German Cancer Research Center, Heidelberg, Germany) [39]. Goat anti-mouse IgG-biotin and Qdot 625-streptavidin were used for detection (Life Technologies).

## RESULTS

### *Activated MiHA-Specific T Cells Can Induce Collateral Damage to Surrounding MiHA-Negative Fibroblasts*

To investigate whether nonhematopoietic tissues that do not express the relevant peptide/HLA complexes can be targeted by the cytotoxic effect of antigen-specific T cells during an ongoing response against antigen-positive hematopoietic target cells, we developed an in vitro model in which HLA-A*0201–positive, MiHA-negative primary human fibroblasts were exposed to $CD8^+$ CTL clones specific for different HLA-A*0201–binding MiHA or $CD4^+$ T cell clones specific for HLA-DP, in the presence or absence of MiHA-positive/HLA-DP–positive hematopoietic stimulator cells. We first examined the direct cytotoxic activity of the MiHA-specific CTLs against the single targets and confirmed that no direct antigen-specific kill of MiHA-negative targets was seen after 24 hours (Figure 1A). As control, it was demonstrated that the CTLs specific for the ubiquitously expressed MiHA LB-ADIR-1F and SMCY-HY showed efficient lysis of MiHA-positive fibroblasts and EBV-LCL, demonstrating their functional potency (Figure 1A). As expected, T cells targeting the hematopoiesis-restricted MiHA HA-1 and the $CD4^+$ T cell clones targeting HLA-DP killed only the MiHA/HLA-A*0201–positive or HLA-DP–positive EBV-LCL, respectively, but not the fibroblasts, owing to the lack of expression of both HA-1 and HLA class II on the fibroblasts.

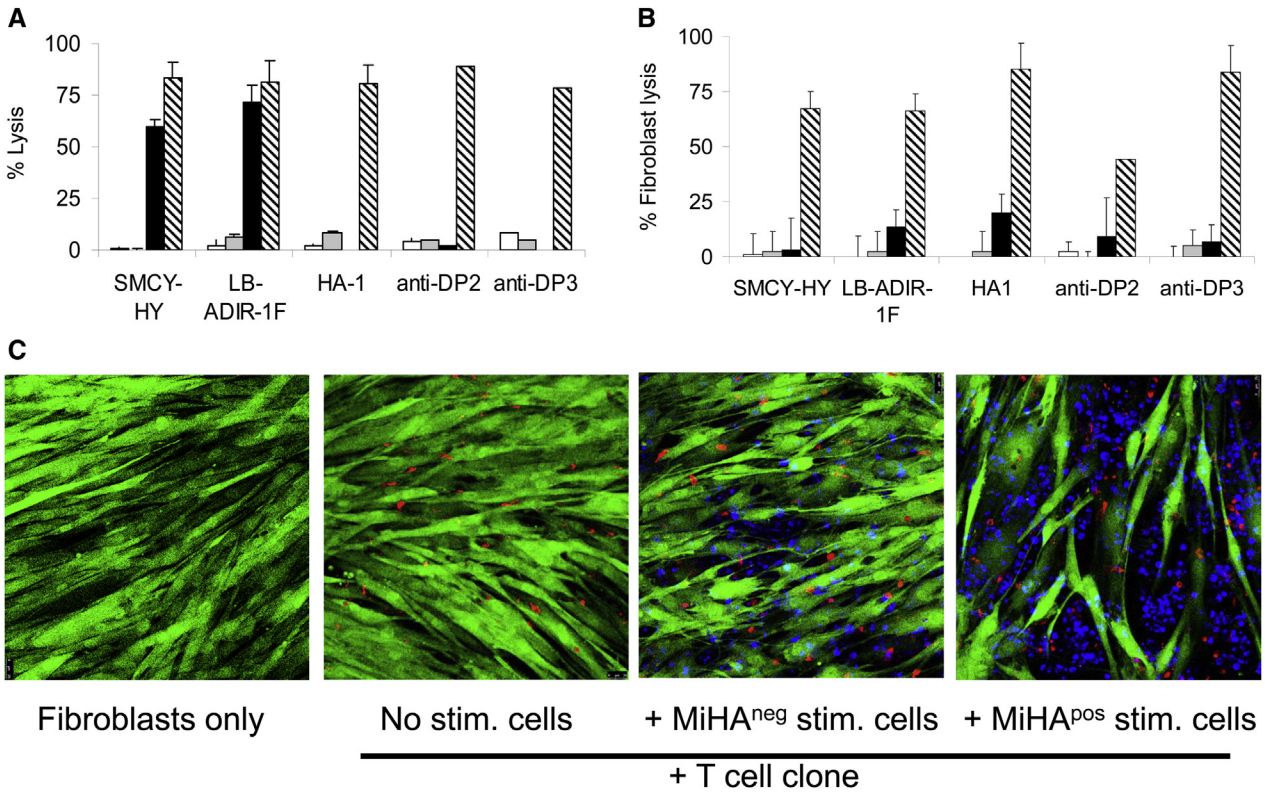


**Figure 1.** Activated alloreactive T cells can induce collateral damage to surrounding antigen-negative fibroblasts. Cytotoxicity against primary human fibroblasts by different MiHA- and allo-HLA–specific T cell clones (CTLs) was analyzed by quantitative FACS analysis after 24 hours of coincubation. (A) HLA-A*0201–restricted $CD8^+$ CTL clones directed against MiHA SMCY-HY and LB-ADIR-IF exerted direct cytotoxic activity against HLA-A*0201–positive, MiHA-positive fibroblasts (●) and MiHA-positive EBV-LCL (⊘), but not against HLA-A*0201–positive, MiHA-negative fibroblasts (○) or HLA-A*0201–positive, MiHA-negative EBV-LCL (◌) (effector cell:target cell ratio, 5:1). As expected, the CD8 clone recognizing the hematopoiesis-restricted MiHA HA-1 and the HLA-DP2– and HLA-DP3–specific CD4 T cell clones exerted cytotoxic activity only against MiHA/HLA-A*0201–positive and HLA-DP2/3–positive EBV-LCL, respectively (⊘), and not against the fibroblasts (●), owing to a lack of expression of both HA-1 and class II on the fibroblasts. Data shown are mean ± SD of 3 replicates from a representative of at least 3 independent experiments. (B) No collateral damage to HLA-A*0201–positive, MiHA/HLA-DP2/3–negative fibroblasts was induced by MiHA-specific $CD8^+$ T cells (SMCY-HY, LB-ADIR-1F, and HA-1) or HLA-DP2/3–specific CD4 T cells (fibroblast:T cell ratio, 1:5) in the absence of third-party stimulator cells (○) and in the presence of MiHA/HLA-DP2/3–negative EBV-LCL (●) (T cell:EBV-LCL ratio, 1:3). Introduction of MiHA/HLA-DP2/3–positive EBV-LCL as third-party stimulator cells resulted in collateral damage to the surrounding fibroblasts (⊘) (T cell:EBV-LCL ratio, 1:3). As a control, the MiHA/HLA-DP2/3–positive EBV-LCL were added to the fibroblasts in the absence of T cell clones. This did not result in lysis of the fibroblasts (◌). Data shown are mean ± SD of 3 replicates from a representative of at least 3 independent experiments. (C) Visualization of collateral damage induction to GFP-positive (green) fibroblasts by PKH26-labeled (red) MiHA-specific $CD8^+$ T cells in the presence of CellVue-labeled (blue) MiHA-positive stimulator cells, but not in the absence of stimulator cells or in the presence of MiHA-negative stimulator cells after 72 hours of coincubation (objective HC PL APO 20×/0.700).

To investigate whether hematopoiesis-specific T cells activated by hematopoietic stimulator cells can induce bystander lysis to surrounding nonhematopoietic cells, we added MiHA-positive stimulator cells to the system as third-party cells. Thus, MiHA-specific T cells seeded on a monolayer of MiHA-negative fibroblasts were challenged with MiHA-negative or MiHA-positive stimulator cells. MiHA-specific CTLs and HLA-DP-specific CD4 T cells were capable of inducing collateral damage to the surrounding MiHA/HLA-DP–negative fibroblasts only when stimulator cells expressing the relevant HLA/MiHA complexes were added to the system (Figure 1B). This phenomenon was confirmed by confocal fluorescent microscopy visualization of loss of GFP-labeled MiHA-negative fibroblasts by PKH26-labeled MiHA-specific CTLs in the presence of CellVue-labeled HLA-A*0201/MiHA-positive stimulator cells, whereas no reduction in the number of viable fibroblasts was observed in the absence of third-party stimulator cells or after the addition of MiHA-negative stimulator cells (Figure 1C). These data indicate that induction of collateral damage to surrounding MiHA-negative fibroblasts is induced only after local T cell activation.

### *Strength of Local T Cell Activation by MiHA-Positive Stimulator Cells Correlates with the Degree of Collateral Damage to Surrounding MiHA-Negative Fibroblasts*

We investigated whether collateral damage can be induced when T cells are stimulated with other clinically relevant targets using different primary hematopoietic stimulator cells. Collateral damage to MiHA-negative fibroblasts was induced by HLA-A*0201–restricted, MiHA-specific CTLs on activation with HLA-A*0201/MiHA-positive immature/mature monocyte-derived DCs and ALL cells to the same degree as seen after stimulation with EBV-LCL. Adding the stimulator cells to the fibroblasts in the absence of T cells did not induce collateral damage (Figure 2A). Interestingly, stimulation with HLA-A*0201/MiHA-positive monocytes resulted in only limited induction of collateral damage.

Given that monocytes are known to be less potent antigen-presenting cells (APCs), we examined the degree of T cell activation after coincubation with the different targets in the absence of fibroblasts. Strong IFN-γ production on encountering all HLA-A*0201/MiHA-positive hematopoietic targets was observed, with the exception of stimulation with

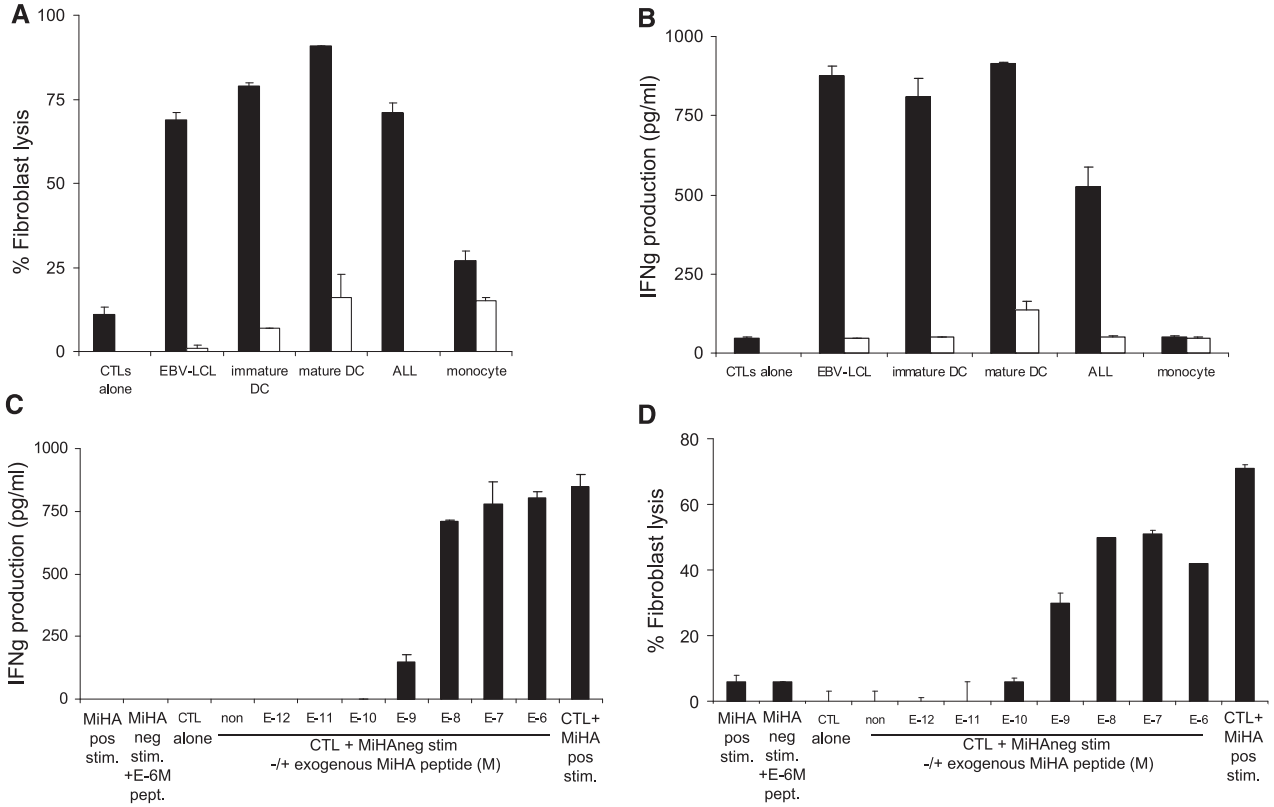


**Figure 2.** The strength of local T cell activation dictates the degree of collateral damage to surrounding nonhematopoietic cells. MiHA-specific T cells seeded on a monolayer of HLA-A*0201–positive, MiHA-negative fibroblasts were activated using different stimulator cells. The resulting fibroblast lysis was evaluated by quantitative FACS analysis, and T cell activation was analyzed by IFN-γ ELISA. (A) Activation of MiHA-specific CTLs seeded on a monolayer of HLA-A*0201–positive, MiHA-negative fibroblasts (CTL:fibroblast ratio, 5:1) with different HLA-A*0201–positive, MiHA-positive hematopoietic stimulator cells (●) (CTL:stimulator cell ratio, 1:3) resulted in collateral damage to the surrounding fibroblasts. As a control, the stimulator cells were added to the fibroblast monolayer in the absence of T cells. This did not result in fibroblast lysis (○). Representative results are shown for the HA-1–specific CTLs; similar results were obtained with other MiHA-specific CTLs. (B) Stimulation of the MiHA-specific T cells with MiHA-positive EBV-LCL, mature and immature DCs, or ALL cells resulted in profound IFN-γ production (●), but stimulation with MiHA-positive monocytes did not. IFN-γ production by the stimulator cells alone (without T cells) is shown as a control (○). Representative results are shown for the HA-1–specific CTLs; similar results were obtained with other MiHA-specific CTLs. (C) Stimulation of MiHA-specific CTLs with HLA-A*0201–positive, MiHA-negative ALL cells exogenously loaded with increasing concentrations of the MiHA peptide or with HLA-A*0201–positive, MiHA-positive ALL cells resulted in dose-dependent activation, as reflected by IFN-γ production. Representative results are shown for the LB-ADIR-1F–specific CTLs. Similar results were obtained with other MiHA-specific CTLs. (D) Stimulation of MiHA-specific CTLs seeded on a monolayer of HLA-A*0201–positive, MiHA-negative fibroblasts with HLA-A*0201–positive, MiHA-negative ALL cells loaded exogenously with increasing concentrations of the MiHA peptide or with HLA-A*0201–positive, MiHA-positive ALL cells resulted in dose-dependent lysis to the surrounding fibroblasts. Representative results are shown for the LB-ADIR-1F–specific CTLs; similar results were obtained with other MiHA-specific CTLs.

monocytes (Figure 2B), which correlated with the observed differential levels of coinciding collateral damage.

To investigate whether the strength of T cell activation correlated with the degree of collateral damage, we used HLA-A*0201–positive/MiHA-negative stimulator cells exogenously loaded with increasing concentrations of the relevant MiHA peptide to stimulate MiHA-specific CTLs seeded on a monolayer of MiHA-negative fibroblasts. Dose-dependent activation of the MiHA-specific CTL clone was observed, as reflected by increasing levels of IFN-γ production (Figure 2C), and the amount of collateral damage to the fibroblasts showed a similar dose-dependent increase on exogenous peptide loading of the stimulator cells (Figure 2D). These data illustrate that the strength of local activation of the T cells dictates the degree of collateral damage to the surrounding fibroblasts.

### *Collateral Damage Is Not Mediated via Cross-Presentation of Peptide/HLA Complexes*

Given the known ability of APCs to capture and present exogenous peptides or even complete peptide/HLA complexes from (dying) third-party cells [40-42], we investigated whether the observed collateral damage to HLA-A*0201–positive/MiHA-negative fibroblasts was related to cross-presentation of MiHA peptides released by the dying MiHA-positive stimulator cells. We first examined the effect of expression of HLA-A*0201 by the fibroblasts on the level of collateral damage induced by HLA-A*0201–restricted MiHA-specific CTLs. Similar levels of collateral damage were induced in both HLA-A*0201–positive and HLA-A*0201–negative MiHA-negative fibroblasts. Moreover, no collateral damage was observed when HLA-A*0201–negative/MiHA-positive EBV-LCL were added to the system as third-party stimulator cells (Figure 3A). These data illustrate that cross-presentation of MiHA/HLA complexes taken up from (dying) stimulator cells is not the dominant mechanism underlying the induction of collateral damage to the surrounding fibroblasts.

To investigate the capability of CTLs to induce collateral damage in a system in which cross-presentation is impossible, we developed a model in which the MiHA-specific CTLs seeded on a monolayer of fibroblasts was activated in a cell-free manner using T cell receptor (TCR) cross-linking by the soluble activator PHA. We demonstrated that local stimulation

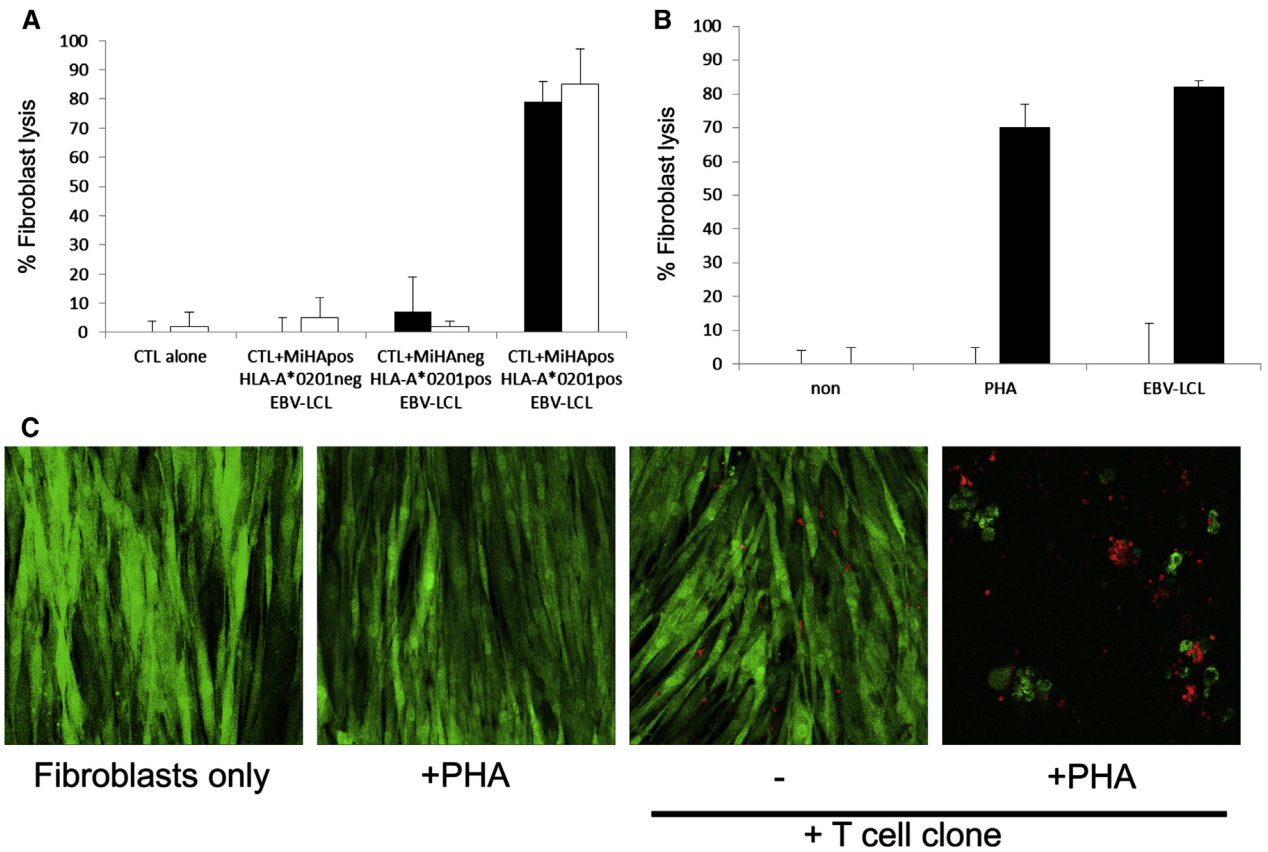


**Figure 3.** Collateral damage is not mediated by cross-presentation of peptide/HLA complexes. To investigate whether cross-presentation of peptides or peptide/HLA complexes derived from MiHA-positive stimulator cells was the underlying mechanism for collateral damage to MiHA-negative fibroblasts by MiHA-specific CTLs, we incubated MiHA-negative fibroblasts either expressing or not expressing the HLA-A*0201 restriction molecule of the MiHA-specific CTLs, and then activated the CTLs with third-party stimulator cells or in a cell-free system. (A) HLA-A*0201–restricted MiHA-specific CTLs were seeded on a monolayer of MiHA-negative, HLA-A*0201–negative (●) or HLA-A*0201–positive (○) fibroblasts. Collateral damage to the surrounding fibroblasts was induced on stimulation of the MiHA-specific CTLs with HLA-A*0201–positive, MiHA-positive EBV-LCL irrespective of the expression of HLA-A*0201 by the fibroblasts. (B) Activation of MiHA-specific CTLs seeded on a monolayer of MiHA-negative fibroblasts using PHA in the absence of third-party stimulator cells resulted in similar levels of collateral damage induction to the surrounding fibroblasts, as seen after stimulation with third-party MiHA-positive EBV-LCLs (●). No damage to the fibroblasts was seen after incubation with either PHA or the MiHA-positive EBV-LCL in the absence of CTLs (○). (C) Induction of collateral damage to MiHA-negative GFP-labeled fibroblasts (green) by PKH-26–labeled MiHA-specific CTLs (red) on stimulation with PHA was visualized by confocal microscopy (Hc PL APO CS 10×/0.4 dry objective, 4× zoom). Representative results are shown for the HA-1–specific CTLs; similar results were obtained with the other MiHA-specific CTLs.

of the CTLs with PHA in the absence of third-party stimulator cells resulted in very profound induction of collateral damage to the surrounding MiHA-negative fibroblasts, whereas the addition of PHA in the absence of T cells did not affect the fibroblasts (Figure 3B and C). This profound induction of collateral damage to surrounding MiHA-negative fibroblasts on local stimulation of the CTLs in an activation model free of third-party stimulator cells allowed us to analyze the underlying effector mechanisms in detail.

### *When Properly Activated, Primary Human T Cells Can Induce Collateral Damage to Surrounding Antigen-Negative Fibroblasts*

Because the PHA stimulation model is not influenced by the fine specificity of the T cells, this model allowed us to use polyclonal primary T cell populations instead of T cell clones. $CD8^+$ and $CD4^+$ memory and naïve primary T cells were able to induce collateral damage to surrounding fibroblasts after PHA stimulation. Importantly, no damage to the fibroblasts was induced by the primary T cell populations in the absence of PHA, thus excluding the role of alloreactivity in these experiments (Figure 4). These data further illustrate that on profound local activation, any T cell can cause collateral damage to surrounding nonhematopoietic cells.

### *Direct Contact between Activated T Cells and Fibroblasts Is Required for Induction of Collateral Damage*

To investigate whether collateral damage can be induced when the T cells are in proximity to but not in direct contact with the fibroblasts, we first analyzed whether soluble factors produced by the activated MiHA-specific T cells can mediate the induction of collateral damage to the MiHA-negative fibroblasts. To do so, we exposed the fibroblasts to supernatants harvested from cocultures of MiHA-specific CTLs and MiHA-positive stimulator cells. Although significant levels of secreted perforin and granzyme B were present in the supernatants from CTLs stimulated with PHA or MiHA-positive EBV-LCL, exposure to these supernatants did not induce fibroblast lysis. Separation of the activated T cells and fibroblasts in a Transwell system prevented the induction of collateral damage, whereas in the positive control, coculture of the 3 cell types in the same compartment resulted in induction of collateral damage (Figure 5A and B). These data illustrate that profound activation of T cells in relative proximity of the fibroblasts does not lead to induction of collateral damage to surrounding fibroblasts.

To further investigate whether full cell–cell contact is necessary, we developed a model in which we could increase and decrease the level of cell–cell contact between the activated T cells and the fibroblasts. We added cell-sized CD3/28 stimulation beads to nearly confluent monolayers of fibroblasts and preattached T cells. Whereas in the absence of the CD3/28 beads, almost all CTLs were in close contact with the fibroblasts, adding the CD3/28 beads to the T cell/fibroblast monolayer resulted in attraction of the T cells and significantly reduced T cell–fibroblast interaction, as reflected in the decreased number of T cells showing red fluorescence at the fibroblast level and the increased number of T cells interacting with the beads showing red fluorescence above the fibroblast monolayer (Figure 5C). This CD3/28-induced activation of the T cells in very close proximity to the confluent fibroblast layer did not lead to induction of collateral damage. In contrast, when all components (cells and beads/PHA) were brought together in suspension, allowing direct cell–cell contact between the activated T cells and the fibroblasts, clear collateral damage was observed, although the level of T cell activation as measured by IFN-γ production was similar in the 2 conditions (Figure 5D and E).

Considering that ICAM-1 expression is known to be a key factor in the interaction between T cells and fibroblasts [26,43,44], we investigated whether we could prevent collateral damage induction by blocking T cell–fibroblast interaction using ICAM-1– blocking mAb. ICAM-1 blockade significantly decreased the level of collateral damage (Figure 5F). These data illustrate that besides profound activation, direct cell–cell contact between the activated T cells and the fibroblasts is critical for the induction of collateral damage, and that this interaction is mediated, at least in part, by ICAM-1.

### *Misdirection of Cytotoxic Granule Release Leads to Induction of Collateral Damage via the Classical Apoptotic Pathway*

To investigate the exact effector mechanism responsible for the induction of collateral damage, we studied the kinetics of fibroblast death in more depth by staining with SYTOX, a dye taken up solely by dead cells with disintegrated membranes, and by annexin V staining as a marker for apoptosis induction. Although morphological changes in the fibroblasts were already observed within 3 hours after local T cell activation, no end-stage SYTOX-positive dead cells were observed at that point. At 20 hours after local T cell activation, all fibroblasts had died, as demonstrated by their complete disappearance and SYTOX staining of the remnants (Figure 6A). Interestingly, within 3 hours after local T cell stimulation, surrounding fibroblasts showed positive annexin V staining, demonstrating early initiation of the apoptosis process, whereas no annexin V–positive fibroblasts were detected when fibroblasts were cultured alone or with unstimulated T cells (Figure 6B). These data illustrate that although immediate initiation of the apoptosis process in the fibroblasts can be seen after local T cell activation, it takes time before the fibroblasts are truly dead, as demonstrated by disintegration of their outer cell membranes.

To investigate whether we could identify the apoptotic pathway responsible for collateral damage induction, we increased the expression of inhibitors of the 3 main apoptotic

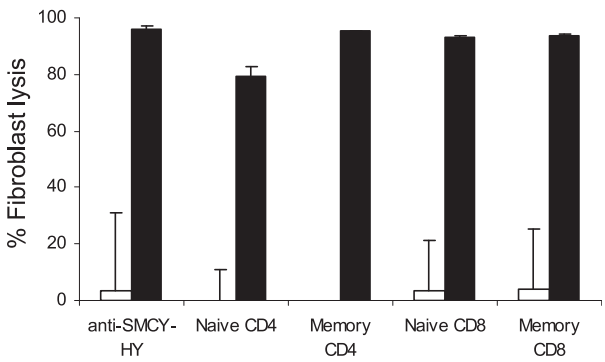


**Figure 4.** Primary human T cells induce collateral damage to surrounding nonhematopoietic cells on vigorous local activation. Selected populations of naïve and memory CD8 and CD4 primary T cells were isolated from peripheral blood of healthy donors and seeded on monolayers of human fibroblasts (T cell:fibroblast ratio, 5:1). Whereas no direct (alloreactive) cytotoxicity was induced against the fibroblasts without stimulation of the T cells (○), clear induction of fibroblast lysis was observed after activation with PHA (●). The anti–SMCY-HY CD8 CTL clone served as a control.

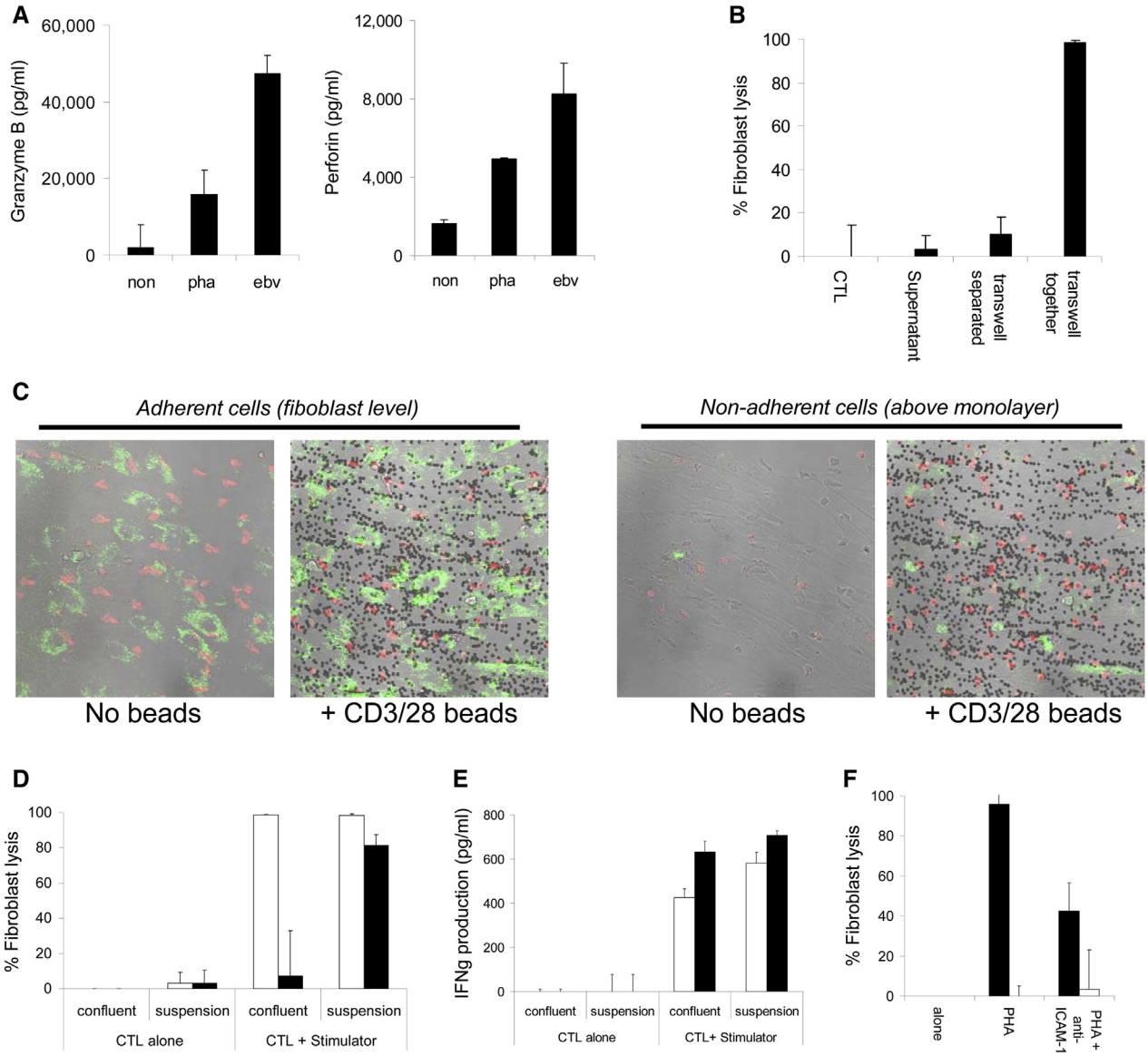


**Figure 5.** Direct contact between the activated T cells and the fibroblasts is required for the induction of collateral damage. To investigate the need for direct cell–cell contact between the activated T cells and the fibroblasts for the induction of collateral damage, we activated the T cells in the neighborhood of or in close proximity of the fibroblasts without direct cell–cell contact, or exposed the fibroblasts to supernatants of activated T cells. (A) Supernatants of an MiHA-specific CTL clone activated with PHA or with MiHA-positive EBV-LCL contained significant amounts of granzyme B and perforin as detected on ELISA. (B) Exposure of the fibroblasts to supernatants of an MiHA-specific CTL clone stimulated with MiHA-positive fibroblasts or separation of the MiHA-negative fibroblasts (lower compartment) and the coculture of MiHA-specific CTLs and MiHA-positive EBV-LCL (upper compartment) in a Transwell system did not result in collateral damage to the MiHA-negative fibroblasts. As a control, MiHA-negative fibroblasts were cocultured with MiHA-specific CTLs and MiHA-positive EBV-LCL in the lower compartment of the Transwell system. This resulted in significant fibroblast lysis. (C) PKH-26–labeled MiHA-specific CTLs (red) were seeded on a monolayer of PKH-67–labeled, CD54-transduced, HLA-A*0201–negative, and MiHA-negative fibroblasts (green) (CTL:fibroblast ratio, 3:1), resulting in strong adherence of the T cells to the fibroblasts after 1 hour of coincubation, as shown by red fluorescence at the fibroblast level and a lack of red fluorescence above the monolayer on confocal microscopy analysis. The addition of T cell–activating CD3/28 microbeads resulted in capture of the T cells from the monolayer, as visualized by diminished red fluorescence at the fibroblast level and increased red fluorescence above the monolayer after 2 hours. This model was used for T cell activation in very close proximity to the fibroblasts. (D) Either MiHA-specific CTLs were seeded on a confluent monolayer of MiHA-negative fibroblasts before activation with PHA (○) or CD3/28 beads (●) (confluent), or the CTLs, fibroblasts, and PHA/CD3/28 beads were added together in suspension, allowing direct cell–cell contact (suspension). On PHA stimulation of the MiHA-specific CTLs, collateral damage to the surrounding fibroblasts clearly occurred under both conditions. In contrast, activation of the MiHA-specific CTLs with CD3/28 beads resulted in induction of collateral damage only when direct cell contact between the T cells and the fibroblasts was allowed (suspension), not when the T cells were captured from the fibroblast monolayer (confluent) and were activated just above the fibroblast monolayer. (E) Similar strength of T cell activation by PHA (○) and CD3/28 beads (●) was observed under both conditions (confluent versus suspension) as measured by IFN-γ ELISA. (F) Blockade of CTL–fibroblast interaction by the addition of anti–ICAM-1 blocking antibodies abrogated the induction of collateral damage to the surrounding fibroblasts on PHA stimulation (●). As a negative control, PHA was added in the absence of CTLs (○).

pathways—cFLIP, PI-9, and Bcl-2—inhibiting the death receptor, granzyme B–mediated, and mitochondrial apoptosis pathways, respectively, in the fibroblasts by retroviral transduction. Steady-state and induced c-FLIP, PI-9, and Bcl-2 protein expression in the fibroblasts was demonstrated by Western blot analysis (Figure 6C). Prevention of collateral damage was not observed in fibroblasts that had been transduced with c-FLIP and Bcl-2, as demonstrated on annexin V staining after coculturing with PHA-activated T cells. In contrast, PI-9 overexpression resulted in clear protection

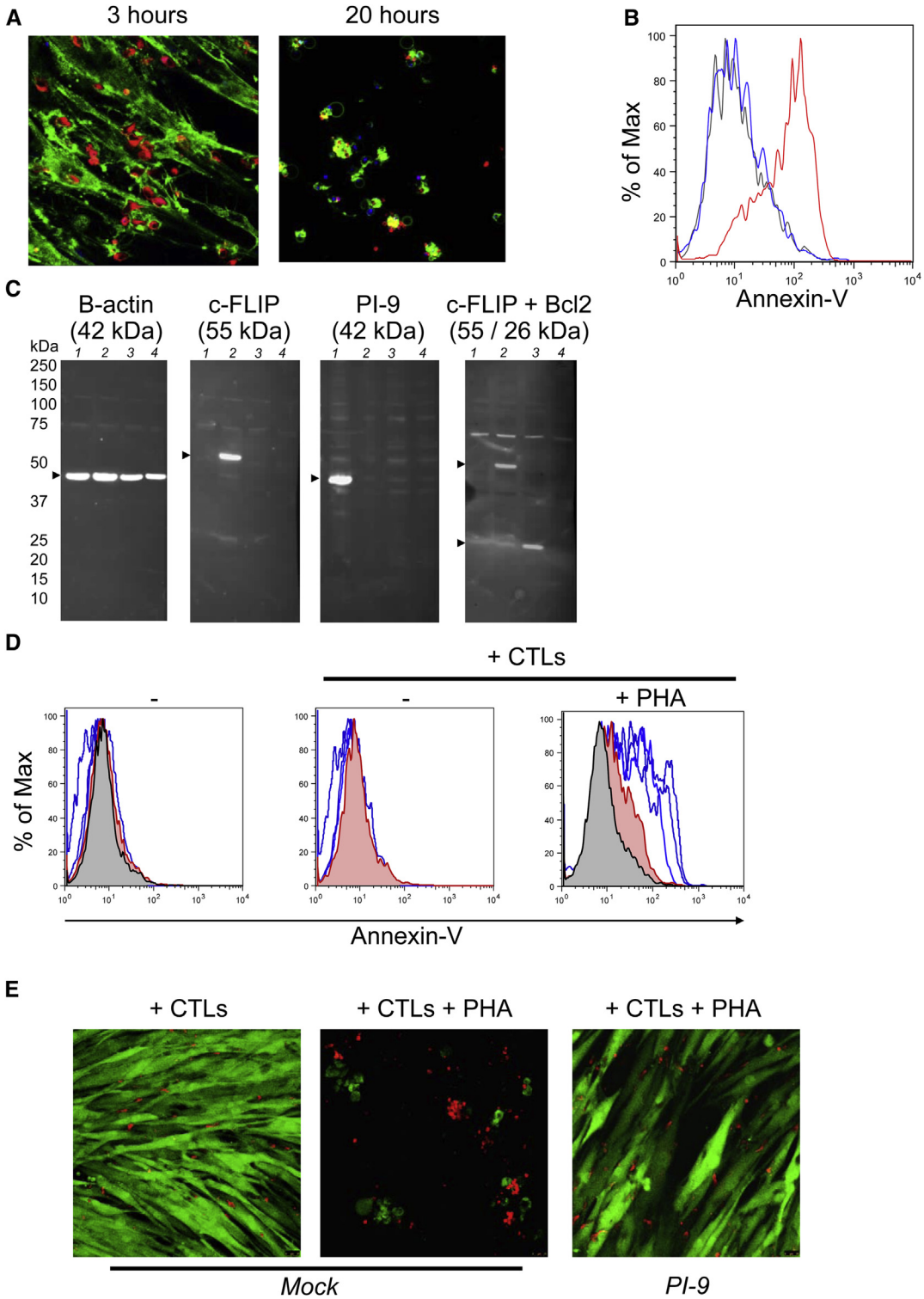


**Figure 6.** Induction of fibroblast apoptosis by misdirection of cytotoxic granule release. The effector mechanism underlying the induction of collateral damage to fibroblasts by locally activated T cells was analyzed in different cell death assays. (A) PKH-26–labeled MiHA-specific CTLs (red) were seeded on a monolayer of FITC-labeled MiHA-negative fibroblasts (green) and activated by the addition of PHA. The death cell staining dye SYTOX (blue) was added to stain end-stage dead cells with a disintegrated cell membrane. Although morphological changes in the fibroblasts were observed as soon as 3 hours after T cell stimulation by confocal fluorescent microscopy, true fibroblast cell death was overt only after 20 hours. The fibroblast cell remnants stained blue with the SYTOX dye (HCX PL APO CS 40×/1.25 oil objective). (B) Apoptosis of GFP-labeled MiHA-negative fibroblasts after coculture with PHA-stimulated MiHA-specific CTLs could be demonstrated after 3 hours by positive staining with annexin V (red line). No annexin V–positive fibroblasts were detected without CTLs (black line) and after coculturing with CTLs in the absence of PHA (blue line). The histograms are gated on GFP-positive cells. (C) Expression of the inhibitors of the main apoptosis pathways c-FLIP, PI-9, and Bcl-2 was increased by retroviral transduction. Endogenous and up-regulated expression after transduction was evaluated by Western blot analysis. Lane 1 shows PI-9–transduced fibroblasts, lane 2 shows c-FLIP–transduced fibroblasts, lane 3 shows Bcl-2–transduced fibroblasts, and lane 4 shows empty vector (mock)-transduced fibroblasts. Staining with the Bcl-2 antibody was performed on the c-FLIP–prestained blot. Arrows indicate the specific bands. (D) Apoptosis of GFP-labeled fibroblasts by PHA-stimulated T cells was observed in mock-, Bcl-2–, and c-FLIP–transduced fibroblasts (blue lines). Apoptosis induction was prevented in PI-9–transduced fibroblasts (red histograms) and by the addition of EGTA (gray histograms). No induction of apoptosis was observed without CTLs or after coculture with CTLs in the absence of PHA stimulation. Annexin V staining gated on GFP-positive cells is shown after a 3-hour incubation. (E) Clear induction of fibroblast cell death was observed in GFP-labeled mock-transduced MiHA-negative fibroblasts (green) after 40 hours of coculture with PHA-stimulated PKH-26–labeled MiHA-specific CTLs (red) as visualized by confocal microscopy (Hc PL APO CS 10×/0.4 dry objective, 4× zoom). Fibroblast lysis by PHA-stimulated CTLs was abrogated by overexpression of PI-9.

from collateral damage, as reflected by a decreased amount of annexin V–positive fibroblasts (Figure 6D). This PI-9–mediated protection against collateral damage was confirmed by visualization with confocal microscopy (Figure 6E). Taken together, these data demonstrate that granzyme B released from the CTL granules plays a key role in the induction of collateral damage to surrounding nonhematopoietic cells.

To further demonstrate the role of cytotoxic granule release by the activated T cells, we examined the effect of inhibition of calcium-dependent degranulation by the addition of EGTA. Prevention of T cell degranulation by the addition of EGTA to the coculture of fibroblasts and PHA-activated T cells abrogated the induction of collateral damage (Figure 6D). Taken together, these data suggest that collateral damage is induced by misdirection of cytotoxic granules released by activated T cells, resulting in granzyme B–mediated apoptosis induction in surrounding nonhematopoietic cells when they are in direct contact with the T cells.

## DISCUSSION

The aim of the present study was to investigate whether and, if so, under which conditions T cells recognizing MiHA with a hematopoiesis-restricted expression pattern may be able to induce damage to nonhematopoietic targets, thereby contributing to the amplification of a GVHD response that often coincides with the induction of profound GVL responses after allo-SCT and DLI. We developed different in vitro models to mimic the complex immunologic situation after allo-SCT and to analyze in detail the interaction between antigen-specific T cells and nonhematopoietic primary human skin–derived fibroblasts that do not express the antigens targeted by the T cells. We have demonstrated that collateral damage to neighboring nonhematopoietic cells could be induced by virtually every memory/naïve CD4/CD8 T cell that is profoundly locally activated.

Induction of apoptosis via granzyme B released from the activated T cells was the key mechanism, and stringent adhesion between the T cell and the fibroblast was a prerequisite for this collateral damage to occur. We found that collateral damage was not induced by cross-presentation of MiHA peptides or by peptide/MHC complexes taken up by the fibroblasts from dying MiHA-positive stimulator cells. These data illustrate that along with antigen-specific direct cytotoxicity by alloreactive T cells recognizing antigens expressed on nonhematopoietic cells and amplification of the damage by the overwhelming cytokine storm coinciding with this antigen-specific immune response [45], under specific circumstances, damage to nonhematopoietic cells also may occur through the induction of bystander lysis by locally activated T cells.

Profound grade III-IV acute GVHD after allo-SCT is thought to be caused by generalized damage induced by alloreactive T cells massively infiltrating tissues and organs and recognizing antigens expressed in these tissues and organs, amplified by a cytokine storm accompanying the immune response. Such generalized severe acute GVHD is particularly prevalent after non–T cell–depleted allo-SCT using HLA-mismatched transplants. This is also the type of GVHD that is nicely demonstrated in skin explant models using male (HY)-specific T cells [14].

GVHD also can present in a more localized fashion, however. Localized infiltration of T cells can lead to patchy fields of inflammatory cells within a heterogeneous cellular composition in tissues. In contrast to generalized GVHD, the extent of this local presentation of GVHD appears to be somewhat controlled and thus is unlikely to be induced by T cells recognizing antigens that are broadly expressed by all nonhematopoietic cells. This form of local patchy modest GVHD is frequently observed, especially in the more controlled setting of T cell–depleted allo-SCT. We hypothesize that under these circumstances, the phenomenon of collateral damage induction described in this article may play a role. For instance, tissue-resident groups of patient-derived hematopoietic APCs may result in local activation of patrolling donor-derived T cells and induction of collateral damage to neighboring nonhematopoietic cells. The extent of the damage will depend on the absolute numbers/local proliferation of patient-derived APCs and donor-derived T cells, but the nature of and presentation of this form of GVHD suggests that it is not caused by direct toxicity exerted by alloreactive T cells recognizing antigens expressed on the nonhematopoietic cells, but more likely is induced by a toxic bystander lysis effect caused by locally activated T cells. Given that the frequencies of potential alloreactive T cells are dictated by the number of genetic differences between donors and recipients, the use of unrelated donors likely will increase the risk.

In essence, every T cell, including virus- and tumor-specific CD8/CD4 T cells, harbors the potential to induce collateral damage to bystander cells, as demonstrated in different in vitro models by us and others [15-25]. This property may imply that collateral damage to nonhematopoietic cells can occur even when allo-SCT recipients are treated with selected populations of donor T cells directed against antigens expressed exclusively on (malignant) hematopoietic cells. Although this is not likely to result in overt massive damage as is seen in acute GVHD after non–T cell–depleted allo-SCT, local induction of a profound hematopoiesis-specific immune response may result in bystander lysis of neighboring nonhematopoietic cells. This possibility fits with the clinical observations reported in patients with significant levels of malignant cells at the moment of onset of the GVL response, when induction of a profound GVL response often coincides with limited, local signs of GVHD, that mismatching for hematopoiesis-restricted MiHAs like HA-1 in the allotransplantation setting is still associated with GVHD, as well as with the significant, albeit modest (grade II), GVHD reactivity seen in skin explant models using HA-1– and HA-2–specific T cells [12-14]. In the situation of local presentation of virus infections in specific organs such as the gut or lungs (cytomegalovirus disease), virus-specific T cells also may cause local damage, not only via direct toxicity against virus-infected cells, but also by amplification of the damage via the induction of collateral damage. Although fibroblasts are not generally assumed to be the primary target cell for acute GVHD, our findings indicate that the susceptibility to collateral damage is a common phenomenon in different nonhematopoietic target cell types. We were able to demonstrate similar induction of collateral damage to in vitro cultures of adherent tumor cell lines and keratinocytes (data not shown), indicating that T cells may cause local damage in tissues and organs via the mechanism of collateral damage.

In conclusion, our findings suggest that under specific conditions, antigen-specific T cells may cause off-target toxicity through induction of collateral damage to neighboring antigen-negative cells. This toxicity may play a role in the induction and/or amplification of GVHD after allo-SCT and DLI.

## ACKNOWLEDGMENTS

The authors thank Annelies Boonzaaier-van der Laan and Joop Wiegant, Department of Molecular Cell Biology, Leiden University Medical Center, The Netherlands, for their expert technical assistance with the confocal microscopy analysis.

*Financial disclosure:* This work was supported by the Dutch Cancer Society (UL 2007-3905).

*Conflict of interest statement:* There are no conflicts of interest to report.

## REFERENCES

1. Appelbaum FR. The current status of hematopoietic cell transplantation. *Annu Rev Med*. 2003;54:491-512.
2. Kolb HJ. Graft-versus-leukemia effects of transplantation and donor lymphocytes. *Blood*. 2008;112:4371-4383.
3. Falkenburg JH, van de Corput L, Marijt EW, Willemze R. Minor histocompatibility antigens in human stem cell transplantation. *Exp Hematol*. 2003;31:743-751.
4. Feng X, Hui KM, Younes HM, Brickner AG. Targeting minor histocompatibility antigens in graft versus tumor or graft versus leukemia responses. *Trends Immunol*. 2008;29:624-632.
5. Mullally A, Ritz J. Beyond HLA: the significance of genomic variation for allogeneic hematopoietic stem cell transplantation. *Blood*. 2007;109:1355-1362.
6. Irle C, Beatty PG, Mickelson E, et al. Alloreactive T cell responses between HLA-identical siblings: detection of anti-minor histocompatibility T cell clones induced in vivo. *Transplantation*. 1985;40:329-333.
7. Riddell SR, Murata M, Bryant S, Warren EH. Minor histocompatibility antigens: targets of graft-versus-leukemia responses. *Int J Hematol*. 2002;76(Suppl 2):155-161.
8. Riddell SR, Berger C, Murata M, et al. The graft-versus-leukemia response after allogeneic hematopoietic stem cell transplantation. *Blood Rev*. 2003;17:153-162.
9. Aglietta M, Piacibello W, Stacchini A, et al. Expression of HLA class II (DR, DQ) determinants by normal and chronic myeloid leukemia granulocyte/monocyte progenitors. *Cancer Res*. 1986;46(4 Pt 1):1783-1787.
10. Ibisch C, Gallot G, Vivien R, et al. Recognition of leukemic blasts by HLA-DPB1–specific cytotoxic T cell clones: a perspective for adjuvant immunotherapy post-bone marrow transplantation. *Bone Marrow Transplant*. 1999;23:1153-1159.
11. Rutten CE, van Luxemburg-Heijs SA, Griffioen M, et al. HLA-DP as specific target for cellular immunotherapy in HLA class II–expressing B-cell leukemia. *Leukemia*. 2008;22:1387-1394.
12. Goulmy E, Schipper R, Pool J, et al. Mismatches of minor histocompatibility antigens between HLA-identical donors and recipients and the development of graft-versus-host disease after bone marrow transplantation. *N Engl J Med*. 1996;334:281-285.
13. Tseng LH, Lin MT, Hansen JA, et al. Correlation between disparity for the minor histocompatibility antigen HA-1 and the development of acute graft-versus-host disease after allogeneic marrow transplantation. *Blood*. 1999;94:2911-2914.
14. Dickinson AM, Wang XN, Sviland L, et al. In situ dissection of the graft-versus-host activities of cytotoxic T cells specific for minor histocompatibility antigens. *Nat Med*. 2002;8:410-414.
15. Lanzavecchia A. Is the T-cell receptor involved in T-cell killing? *Nature*. 1986;319:778-780.
16. Gagnon SJ, Ennis FA, Rothman AL. Bystander target cell lysis and cytokine production by dengue virus–specific human CD4(+) cytotoxic T-lymphocyte clones. *J Virol*. 1999;73:3623-3629.
17. Smyth MJ, Krasovskis E, Johnstone RW. Fas ligand–mediated lysis of self bystander targets by human papillomavirus-specific $CD8^+$ cytotoxic T lymphocytes. *J Virol*. 1998;72:5948-5954.
18. Staege MS, Schneider J, Eulitz M, et al. Consequences of antigen self-presentation by tumor-specific cytotoxic T cells. *Immunobiology*. 2000;201:332-346.
19. Gremion C, Grabscheid B, Wolk B, et al. Cytotoxic T lymphocytes derived from patients with chronic hepatitis C virus infection kill bystander cells via Fas–FasL interaction. *J Virol*. 2004;78:2152-2157.
20. Kojima H, Eshima K, Takayama H, Sitkovsky MV. Leukocyte function–associated antigen-1–dependent lysis of $Fas^+$ ($CD95^+$/Apo-$1^+$) innocent bystanders by antigen-specific $CD8^+$ CTL. *J Immunol*. 1997;159:2728-2734.
21. Smyth MJ. Fas ligand–mediated bystander lysis of syngeneic cells in response to an allogeneic stimulus. *J Immunol*. 1997;158:5765-5772.
22. Smyth MJ, Sedgwick JD. Delayed kinetics of tumor necrosis factor–mediated bystander lysis by peptide-specific $CD8^+$ cytotoxic T lymphocytes. *Eur J Immunol*. 1998;28:4162-4169.
23. Wang R, Rogers AM, Ratliff TL, Russell JH. CD95-dependent bystander lysis caused by $CD4^+$ T helper 1 effectors. *J Immunol*. 1996;157:2961-2968.
24. Ando K, Hiroishi K, Kaneko T, et al. Perforin, Fas/Fas ligand, and TNF-alpha pathways as specific and bystander killing mechanisms of hepatitis C virus–specific human CTL. *J Immunol*. 1997;158:5283-5291.
25. Kuwano K, Arai S. Involvement of two distinct killing mechanisms in bystander target cell lysis induced by a cytotoxic T lymphocyte clone. *Cell Immunol*. 1996;169:288-293.
26. van der Zouwen B, Kruisselbrink AB, Jordanova ES, et al. Alloreactive effector T cells require the local formation of a proinflammatory environment to allow crosstalk and high-avidity interaction with nonhematopoietic tissues to induce GVHD reactivity. *Biol Blood Marrow Transplant*. 2012;18:1353-1367.
27. de Vries JF, von dem Borne PA, van Luxemburg-Heijs SA, et al. Differential activation of the death receptor pathway in human target cells induced by cytotoxic T lymphocytes showing different kinetics of killing. *Haematologica*. 2007;92:1671-1678.
28. de Vries JF, Wammes LJ, Jedema I, et al. Involvement of caspase-8 in chemotherapy-induced apoptosis of patient derived leukemia cell lines independent of the death receptor pathway and downstream from mitochondria. *Apoptosis*. 2007;12:181-193.
29. Heemskerk MH, de Paus RA, Lurvink EG, et al. Dual HLA class I and class II restricted recognition of alloreactive T lymphocytes mediated by a single T cell receptor complex. *Proc Natl Acad Sci USA*. 2001;98:6806-6811.
30. Jonuleit H, Kuhn U, Muller G, et al. Pro-inflammatory cytokines and prostaglandins induce maturation of potent immunostimulatory dendritic cells under fetal calf serum–free conditions. *Eur J Immunol*. 1997;27:3135-3142.
31. Lee AW, Truong T, Bickham K, et al. A clinical grade cocktail of cytokines and PGE2 results in uniform maturation of human monocyte-derived dendritic cells: implications for immunotherapy. *Vaccine*. 2002;20(Suppl 4):A8-A22.
32. Nijmeijer BA, Szuhai K, Goselink HM, et al. Long-term culture of primary human lymphoblastic leukemia cells in the absence of serum or hematopoietic growth factors. *Exp Hematol*. 2009;37:376-385.
33. van Bergen CA, Kester MG, Jedema I, et al. Multiple myeloma-reactive T cells recognize an activation-induced minor histocompatibility antigen encoded by the ATP-dependent interferon-responsive (ADIR) gene. *Blood*. 2007;109:4089-4096.
34. Meadows L, Wang W, den Haan JM, et al. The HLA-A*0201–restricted H-Y antigen contains a posttranslationally modified cysteine that significantly affects T cell recognition. *Immunity*. 1997;6:273-281.
35. Kloosterboer FM, van Luxemburg-Heijs SA, van Soest RA, et al. Direct cloning of leukemia-reactive T cells from patients treated with donor lymphocyte infusion shows a relative dominance of hematopoiesis-restricted minor histocompatibility antigen HA-1– and HA-2–specific T cells. *Leukemia*. 2004;18:798-808.
36. Stevanovic S, Griffioen M, Nijmeijer BA, et al. Human allo-reactive $CD4^+$ T cells as strong mediators of anti-tumor immunity in NOD/scid mice engrafted with human acute lymphoblastic leukemia. *Leukemia*. 2012;26:312-322.
37. Altman JD, Moss PA, Goulder PJ, et al. Phenotypic analysis of antigen-specific T lymphocytes. *Science*. 1996;274:94-96.
38. Baumann S, Fas SC, Giaisi M, et al. Wogonin preferentially kills malignant lymphocytes and suppresses T-cell tumor growth by inducing PLC$\gamma$1- and $Ca2^+$-dependent apoptosis. *Blood*. 2008;111:2354-2363.
39. Scaffidi C, Medema JP, Krammer PH, Peter ME. FLICE is predominantly expressed as two functionally active isoforms, caspase-8/a and caspase-8/b. *J Biol Chem*. 1997;272:26953-26958.
40. English L, Chemali M, Duron J, et al. Autophagy enhances the presentation of endogenous viral antigens on MHC class I molecules during HSV-1 infection. *Nat Immunol*. 2009;10:480-487.
41. Smyth LA, Harker N, Turnbull W, et al. The relative efficiency of acquisition of MHC:peptide complexes and cross-presentation depends on dendritic cell type. *J Immunol*. 2008;181:3212-3220.
42. Rock KL, Shen L. Cross-presentation: underlying mechanisms and role in immune surveillance. *Immunol Rev*. 2005;207:166-183.
43. Berg NN, Ostergaard HL. Characterization of intercellular adhesion molecule-1 (ICAM-1)-augmented degranulation by cytotoxic T cells: ICAM-1 and anti-CD3 must be co-localized for optimal adhesion and stimulation. *J Immunol*. 1995;155:1694-1702.
44. Symington FW, Santos EB. Lysis of human keratinocytes by allogeneic HLA class I-specific cytotoxic T cells: keratinocyte ICAM-1 (CD54) and T cell LFA-1 (CD11a/CD18) mediate enhanced lysis of IFN-$\gamma$–treated keratinocytes. *J Immunol*. 1991;146:2169-2175.
45. Ferrara JL. Cytokine dysregulation as a mechanism of graft-versus-host disease. *Curr Opin Immunol*. 1993;5:794-799.